PERGAMON

Microelectronics Reliability 42 (2002) 1219–1227

MICROELECTRONICS RELIABILITY

www.elsevier.com/locate/microrel

High resolution AFM scanning Moiré method and its application to the micro-deformation in the BGA electronic package

Huimin Xie [a,*], Anand Asundi [b], Chai Gin Boay [b], Lu Yunguang [b], Jin Yu [b], Zhong Zhaowei [b], Bryan K.A. Ngoi [b]

[a] *Department of Engineering Mechanics, Tsinghua University, 100084 Beijing, China*
[b] *School of Mechanical and Production Engineering, Nanyang Technological University, 639798 Singapore*

Received 30 October 2001; received in revised form 20 March 2002

Abstract

The formation mechanism of atomic force microscope (AFM) Moiré is explained using the transmittance function. The technique for preparing the AFM Moiré specimen grating is described. The sensitivity and accuracy of this method is analyzed. AFM Moiré method is used to measure the thermal deformation ball grid array (BGA) electronic package. The shear strain at the different solders in the BGA package is measured. The result is compared with that from electron beam Moiré method. The consistent comparison result verifies the AFM Moiré method is reliable and effective in the micro-deformation measurement in the electronic package.

1. Introduction

Developments in micro- and nano-engineering need more powerful and lower cost micro-electronics products drawing more emphasis on products electronic packaging. The tendency of the electronic packages is to be smaller, more functional and powerful than ever before. Due to the coexistence of variety materials with different coefficient of thermal expansion, reliability of these packages becomes an interesting problem, especially with smaller package sizes. Thermal mismatches often result in the delamination of interfaces between two materials, which eventually leads to ultimate mechanical and/or electrical failure. Additionally, the field of micro-electro-mechanical systems (MEMS) has been growing rapidly in recent years. Applications range from actuator devices that drive various micro-components including optical mirrors, turbines, linear displacement structures and cantilevers to sensors that detect radiation, magnetic fields and chemical signals. The performance and reliability of these devices strongly depend on the mechanics and materials issues at the micro-scale. It is crucial to understand fundamental aspects of intrinsic stresses, film-substrate adhesion, mechanisms of plastic deformation and fracture in thin films and device structures. The mechanical behavior of MEMS and the failure mechanism of MEMS components become new interesting points for us. In the above mentioned problems, the interface between two materials or components (in the electronic package and MEMS) is in a size from few tens micron to 0.1 mm. Furthermore, the development in nano-technology, nano-machines and components bring many new subjects to mechanics current researcher. Mechanical behavior of nano-structure and component attracts attention of the researchers from materials science and solid mechanics. It is very difficult to utilize the conventional optical methods to measure the deformation in such a small area. Moiré interferometry was employed in the analysis of thermal deformation in electronic packages [1]. When Moiré

* Corresponding author. Address: 133-1104 (133 Unit, Number 1104), Beijing Institute of Technology, 100081 Beijing, China.
E-mail address: mhmxie@sina.com (H. Xie).

0026-2714/02/$ - see front matter
PII: S0026-2714(02)00084-7

interferometer is used to measure a deformation in a micro-area, an objective lens for microscope is utilized to magnify the measured area. However, the magnifying power of the objective lens is fixed, and generally less than $\times 20$. Hence, it is difficult to observe the feature in the measured area with different magnification using this method.

The scanning Moiré method was suggested and advocated by Morimoto [2] from 1980's. In 1996, Read [3] proposed the scanning Moiré method using electron microscope. The scanning lines in the SEM monitor or CCD video camera were utilized as the reference grating to form a scanning Moiré. These results are limited to the deformation measurement by using a grating with a frequency less than 250 lines/mm. Xie [4,5] used the electron beam Moiré and SEM Moiré methods to measure the deformation of a ball grid array (BGA) package with holographic gratings, but the works are confined to measure deformation in micrometer scale. With the development of micro-mechanics and micromachine engineering, new techniques for deformation measurement stepping from micro- to nano-scales are in urgent need.

Atomic force microscope (AFM) scanning Moiré method was proposed to measure the deformation of object from nano- to micrometer scales [6–8], and the formation condition of AFM Moiré pattern was described. However, the relation between displacement and AFM Moiré fringe order is simply analogized from the coarse Moiré method [9,10] in these works. There is further requirement on giving a quantitative derivation on the relation between the displacement and Moiré fringe, and offering an analysis on the measurement sensitivity and accuracy of this method. This paper offers a quantitative explanation on the implication of AFM Moiré. The relation between the displacement and AFM Moiré fringe is directly derived from the transmittance function. The sensitivity and accuracy as well as the adaptability of this method are discussed in detail. The AFM Moiré method was used to measure deformation of a BGA package. The shear strain components at the different solders are measured.

2. Measurement in-plane deformation using the AFM scanning Moiré method

2.1. Formation of the AFM Moiré

The contact mode AFM operates by a scanning tip at the end of a cantilever across the sample surface while monitoring the change in cantilever deflection with a split photodiode detector [11]. When the tip is close enough to the surface of the specimen, the atomic force between the cantilever and the surface of the substrate will lead to deflection of the cantilever. This deflection is transferred into feedback signal. By controlling the force constant, a topographic image corresponding to the surface of the specimen can be displayed in the CRT. The measured area under AFM is adjustable within the maximum scan size of the piezo-scanner. Fig. 1 shows a 0.833 μm spacing holographic grating with a 100 micron piezo-scanner.

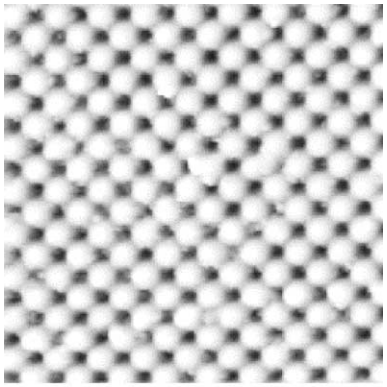

Fig. 1. Configuration of a holographic grating under AFM.

As in Fig. 2, AFM scanning Moiré is formed by the interference between AFM probe scan (reference grating) and the specimen grating. The frequency of the master grating f_r can be defined as

$$f_r = \frac{1}{p_r} = \frac{N}{L} \tag{1}$$

where N is the number of the scanning lines ($N = 64$, 128, 256, 512, ...), L is the scan size, p_r is the pitch of the reference grating.

The transmittance function of reference grating can be expressed as

$$t_1(x,y) = a_0 + a_1 \cos\frac{2\pi}{p_r} y \tag{2}$$

a_0 and a_1 are constants.

Before deformation, the pitch of the specimen grating p_s is assumed to be equal to that of the reference grating. The transmittance function of the specimen grating can be expressed as

$$t_2(x,y) = b_0 + b_1 \cos 2\pi\left[\frac{y}{p_r} + \varphi(x,y)\right] \tag{3}$$

b_0 and b_1 are constants. $\varphi(x,y)$ is the modulation function which is equal to the displacement of the grating lines from its original position divided by the grating period. We have

$$\varphi(x,y) = \frac{v(x,y)}{p_r} \tag{4}$$

where $v(x,y)$ is displacement in y axis.

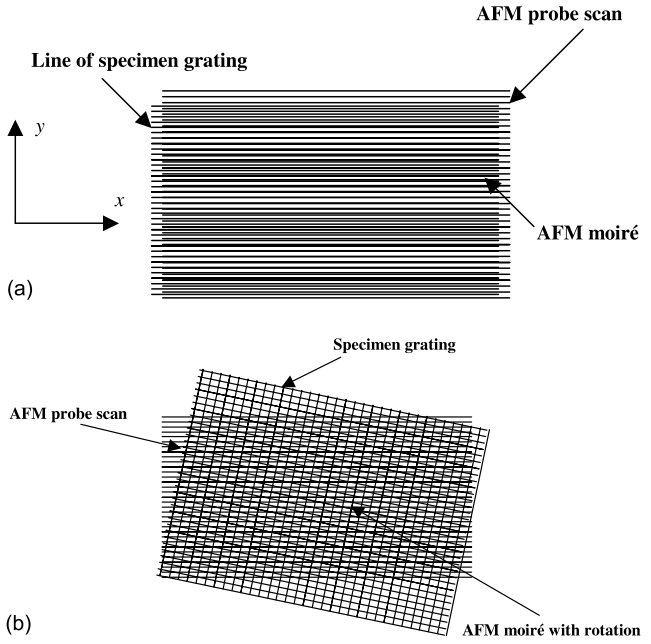

Fig. 2. Formation of AFM scanning Moiré: (a) parallel Moiré and (b) rotation Moiré.

By addition of the two transmittance functions, we have

$$t(x,y) = t_1(x,y) + t_2(x,y) = (a_0 + b_0) + a_1 \cos\frac{2\pi}{p_r} y + b_1 \cos 2\pi\left[\frac{y}{p_r} + \varphi(x,y)\right] \tag{5}$$

When $a_0 = a_1 = b_0 = b_1 = a$, we have

$$t(x,y) = 2a\left\{1 + \cos\pi\varphi(x,y)\cos 2\pi\left[\frac{y}{p_r} + \frac{\varphi(x,y)}{2}\right]\right\} \tag{6}$$

When $\varphi(x,y) = n_v$, $n_v = 0, 1, 2, 3, 4 \ldots$ Eq. (6) reaches a maximum resulting in a bright Moiré fringe.

When $\varphi(x,y) = (2n+1)/2$, $n_v = 0, 1, 2, 3, 4 \ldots$Eq. (6) reaches a minimum resulting in a dark Moiré fringe.

At a bright Moiré fringe line, we have

$$v(x,y) = n_v p_r = \frac{n_v}{f_r} \tag{7}$$

Similarly, when the specimen or the scan direction is rotated by 90° (see as in Fig. 3), we can obtain

$$u = n_u p_r = \frac{n_u}{f_r} \tag{8}$$

where u is the displacement in x-axis, n_u is fringe order of u-field Moiré fringe pattern.

Using Eqs. 7 and 8, the direct strain components $\varepsilon_x, \varepsilon_y$ can be determined as [9,10]

$$\varepsilon_x = \frac{\partial u}{\partial x} = \frac{\partial n_u}{\partial x} p_r \approx \frac{\Delta n_u}{\Delta x} p_r \tag{9}$$

$$\varepsilon_y = \frac{\partial v}{\partial y} = \frac{\partial n_v}{\partial y} p_r \approx \frac{\Delta n_v}{\Delta y} p_r \tag{10}$$

With the Eqs. 7 and 8, the strain component γ_{xy} can be derived as [9,10]

$$\gamma_{xy} = \frac{\partial u}{\partial y} + \frac{\partial v}{\partial x} = \frac{\partial n_u}{\partial y} p_r + \frac{\partial n_v}{\partial x} p_r \approx \frac{\Delta n_u}{\Delta y} p_r + \frac{\Delta n_v}{\Delta x} p_r \tag{11}$$

Before deformation if the pitches of the reference grating and specimen grating are equal, i.e, $p_s = p_r = L/N$, the in-plane strain components ε_x, ε_y, γ_{xy} can be measured using Eqs. (9)–(11).

When $p_s \neq p_r$ before deformation, a carrier Moiré pattern will formed. Ref. [6] offers a condition of generating l orders carrier Moiré fringe in a scan size L, the equation is

$$L = p_s[N \mp (l-1)] \tag{12}$$

Using the carrier Moiré method, the real strain component can be calculated by subtracting the strain components measured from deformed Moiré fringes and the initial carrier Moiré fringes.

2.2. Sensitivity analysis

The sensitivity for displacement measurement with the AFM Moiré method is determined by the number of fringes generated per unit displacement, From Eq. (7),

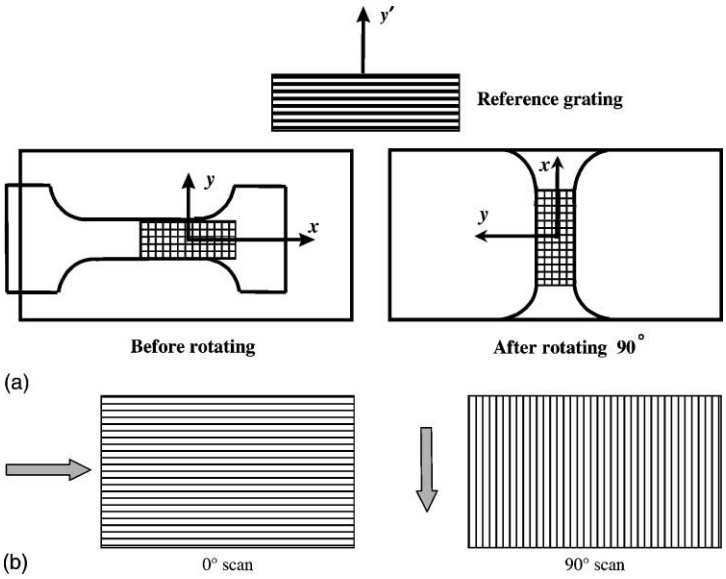

Fig. 3. Two schemes for acquiring $u + v$ filed scanning Moiré patterns: (a) rotation of specimen grating with fixed reference grating; (b) changing of the scan direction with fixed specimen grating.

the sensitivity of displacement measurement SD is equal to the frequency of the reference grating.

$$\mathrm{SD} = \frac{n_v}{v} = f_\mathrm{r} \tag{13}$$

The sensitivity for strain measurement with the AFM Moiré method can be defined as the change of the number of fringes generated per unit strain under a defined scan size., using Eq. (9), Thus, the sensitivity of strain measurement SS can be expressed as

$$\mathrm{SS} = \frac{\Delta n_v}{\varepsilon_y} = \frac{\Delta x}{p_\mathrm{r}} \tag{14}$$

When the scan size is L, $\Delta x = L$, with the Eq. (1), we have

$$\mathrm{SS} = N \tag{15}$$

A sensitivity of direct strain corresponding to scanning line under DI 3000 SPM (Digital Instruments) is shown in Fig. 4.

2.3. Accuracy analysis

From Eq. (9), systemic measurement error for the direct strain can be analyzed. When $\Delta n_u = 1$, we have

$$\left|\frac{\Delta \varepsilon_x}{\varepsilon_x}\right| = \left|\frac{\Delta p_\mathrm{r}}{p_\mathrm{r}}\right| + \left|\frac{\Delta(\Delta x)}{\Delta x}\right| \tag{16}$$

For a 1200 lines/mm grating, if there are three Moiré initial fringe in 20 mm size grating under Moiré inter-

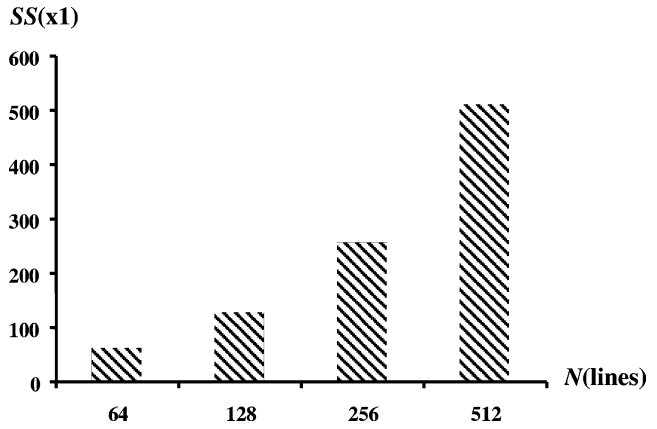

Fig. 4. The relation between the sensitivity of strain measurement SS and the scanning line number N.

ferometer, the relative error from $|\Delta p_r/p_r|$ is smaller than 0.03%. When using Image Tool software to measure the Moiré fringe spacing, $\Delta(\Delta x) = 0.01$ μm, in case the maximum spacing of the Moiré fringe is larger than 0.4 μm, the error from $|\Delta(\Delta x)/\Delta x|$ should be smaller than 2.5%. Finally, the relative measurement error $|\Delta\varepsilon_x/\varepsilon_x|$ can be controlled to be smaller than 2.6%.

When we consider the accuracy of the shear strain measurement, using the Eq. (11), When $\Delta n_u = \Delta n_v = 1$, we have

$$\gamma_{xy} = 2p_r\left(\frac{1}{\Delta y} + \frac{1}{\Delta x}\right) \tag{17}$$

$$\left|\frac{\Delta\gamma_{xy}}{\gamma_{xy}}\right| = \left|\frac{\Delta p_r}{p_r}\right| + \left|\frac{\Delta(\Delta x)}{\Delta x\left(\frac{\Delta x}{\Delta y}+1\right)}\right| + \left|\frac{\Delta(\Delta y)}{\Delta y\left(\frac{\Delta y}{\Delta x}+1\right)}\right| \tag{18}$$

When $\Delta(\Delta y) = 0.01$ μm, and the maximum spacing of the Moiré fringe is larger than 0.4 μm, the error from $|\Delta(\Delta y)/\Delta x|$ should be smaller than 2.5%, thus we have

$$\left|\frac{\Delta\gamma_{xy}}{\gamma_{xy}}\right| = \left|\frac{\Delta p_r}{p_r}\right| + \left|\frac{\Delta(\Delta x)}{\Delta x\left(\frac{\Delta x}{\Delta y}+1\right)}\right| + \left|\frac{\Delta(\Delta y)}{\Delta y\left(\frac{\Delta y}{\Delta x}+1\right)}\right| < \left|\frac{\Delta p_r}{p_r}\right| + \left|\frac{\Delta(\Delta x)}{\Delta x}\right| + \left|\frac{\Delta(\Delta y)}{\Delta y}\right| < 5.1\% \tag{19}$$

2.4. Preparation of AFM Moiré specimen grating

A specimen grating can be manufactured on the measured surface using photolithography method or replication method. By photolithography method, a grating can be directly written on the specimen surface. However, this method requires complicated equipment and special techniques. Specimen grating replication method is a simple approach. A schematic diagram for replicating the specimen grating is shown in Fig. 5.

Before replicating the specimen grating, the measured surface package was cut to expose the measured section using a wire saw. Subsequently, this section surface was polished using fine abrasive paper until measured feature (solders, interface between the materials) became visible and up to 0.02 fineness level. Then the surface was cleaned with ethanol. In the experiment, a 1200 lines/mm grating on ultra-low expansion (ULE) mold plate (deposited with aluminium layer, manufactured by Photomechanics Lab. in Tsinghua University, Beijing, China) was utilized for the replication. The electronic package, and the ULE mold grating were placed in a programmed oven for preheating to 150 °C. TRA BOND-DUCT (TRA-CON, INC) was selected as the adhesive.

The adhesive is pre-heated and then it was mixed with hardener. The mixed adhesive was poured onto the surface of the ULE mold grating. A lens tissue was draped onto the adhesion, and it was dragged across the surface to distribute the adhesion in an uniform thin layer. The preheated specimen was subsequently weighted down onto the adhesion film and left to cure at 150 °C for 2–5 h. After completing the solidification, the specimen was carefully pried off from the ULE mold grating. The aluminium layer with grating was replicated onto the measured surface of the electronic package. Finally, the specimen was cooled down to room temperature. The thermal deformation is recorded in the grating.

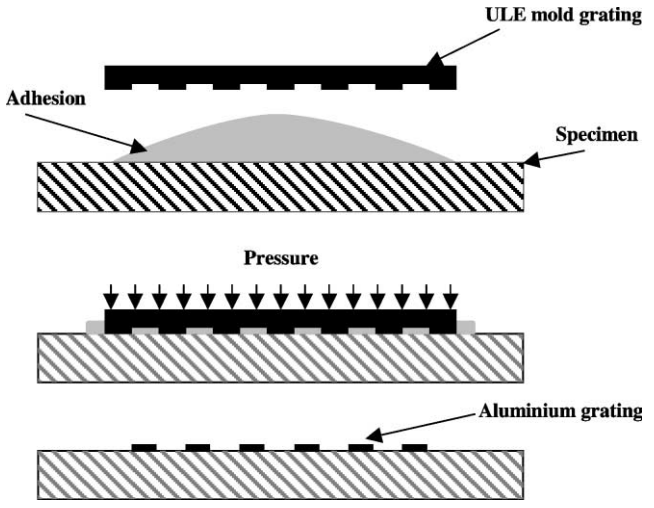

Fig. 5. Procedure of replicating a specimen grating at high temperature.

2.5. Typical test

In order to verify measurement accuracy of the AFM Moiré method, a typical AFM rotation Moiré test was conducted using a standard holographic grating with frequency 1200 lines/mm (cross type) under a DI 3000 SPM. The AFM Moiré patterns were observed under a scan size $L = 100$ μm, scanning line number $N = 128$ with a rotation angle from $-4°$ to $+4°$ (increment = 1°). Rotation Moiré patterns at rotation angle $\theta = 0$, 1°, 2° are shown in Fig. 6. Using the Moiré patterns (from $-4°$ to $+4°$) and Eq. (10), the direct strain ε_y is calculated. The direct strain from different rotation Moiré pattern is listed in Table 1. From this table, it shows that the maximum relative error from these results is smaller than 2.4%.

2.6. Measurement of the thermal deformation BGA electronic package

The thermal deformation of a BGA electronic package was measured using the AFM Moiré method. The BGA package (15 solders, the longitudinal direction is defined as y-axis) was cleaved along the cross section, and the measured area is exposed. After polishing the measured area, a 1200 lines/mm holographic grating on ULE mold plate is replicated on the package at 150 °C using the method as in Section 2.4. The orientation of the solder along the cross section of the package is shown in Fig. 7.

Using the BGA package with the replicated grating, AFM Moiré test was conducted at room temperature. The AFM Moiré was generated with the scanning size $L = 100$ μm and the number of scanning line $N = 256$ under a contact mode AFM. The AFM Moiré patterns of the package at different solders were recorded. Fig. 8 shows the u field Moiré patterns at the center of the solders 1–2 and v field Moiré at the center of the solder 3. Using the recorded Moiré patterns, with Eq. (11), the shear strain γ_{xy} at the different solders was calculated, and the distribution of γ_{xy} according to solders is shown in Fig. 9. These results are compared with the experiment results from the electron beam Moiré method [4], and the comparison illustrates that the maximum relative error between the two corresponding results is smaller than 5%. From Fig. 9, it indicates the values of the shear strain γ_{xy} are varied at the different solder points. At the no. 3 solder strain reaches maximum value. Besides, it

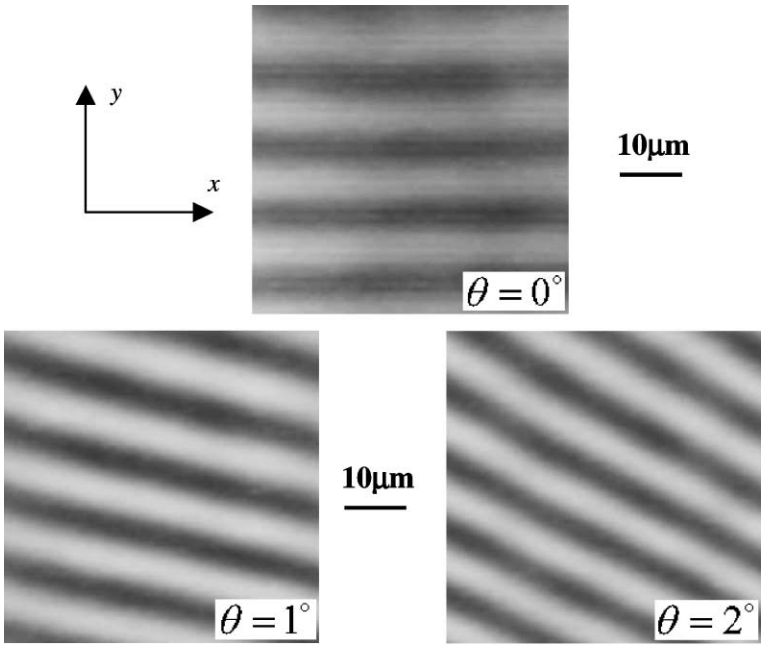

Fig. 6. Rotation Moiré pattern with the different angles.

Table 1
Calculating direct strain ε_y using different rotation Moiré pattern

θ (°)	−4	−3	−2	−1	0	1	2	3	4
$\varepsilon_y(10^{-6})$	1291	1283	1278	1274	1267	1275	1279	1286	1297

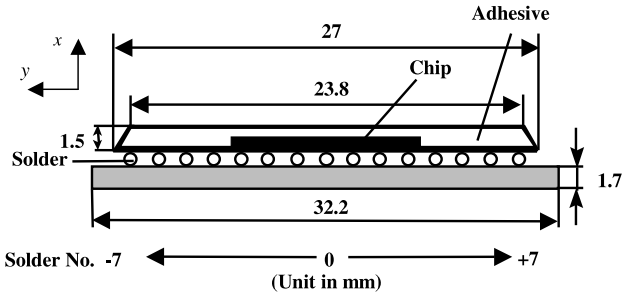

Fig. 7. Schematic diagram of the cross section of the BGA package.

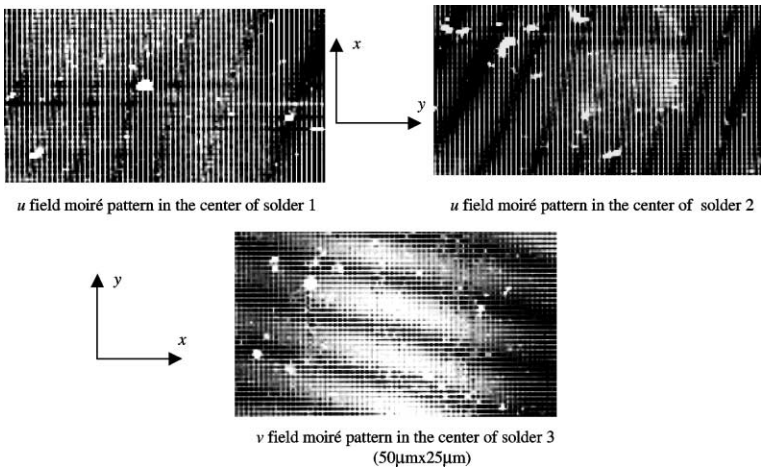

Fig. 8. AFM Moiré fringe patterns at different solders: u field Moiré pattern in the center of solder 1; u field Moiré pattern in the center of solder 2; v field Moiré pattern in the center of solder 3 (50 μm × 25 μm).

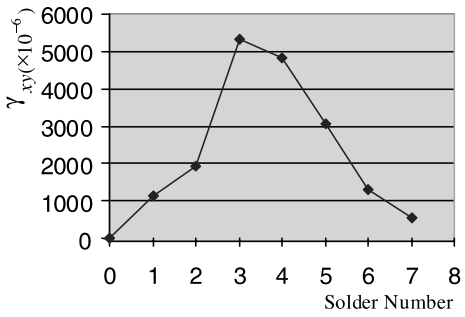

Fig. 9. The distribution of the shear strain γ_{xy} according to the BGA solders.

can be seen that the solder 3 is just located on the boundary of the chip. Because the difference of thermal expansion coefficient between the chip and the circuit board is very large, the solder 3 plays a role as a supporting point. Hence, the average shear strain at this solder is larger than that at other solder points.

3. Analysis and discussion

(1) Before a formal measurement, the AFM should be calibrated to minimize the image distortion. In this study, a STR 10–1800 standard sample is utilized to calibrate 0° and 90° scan, and the image distortion error can be controlled smaller than 5%.

(2) The AFM is usually attached with different piezo-scanners by the manufacturer. For example, 10, 20, 90, 120, 150 micron are the typical size for the scanners. Before experiment, a suitable size for scanner should be determined using Eq. (12). When using a 10^6 lines/mm grating to generate AFM Moiré, 10 or 20 micron scanner should be selected to attain an atomic resolution. As for $N = 128$, the scan size should be selected as 128 or 129 nm, and an initial Moiré fringe pattern with two Moiré fringes could be observed.

(3) Unlike the electron beam Moiré method [3,4] and the SEM scanning Moiré method [2,5], the AFM Moiré method can easily change the direction of the reference grating by converting scan angle. And thus, it is

Fig. 10. A nano-Moiré pattern formed by the lattice of mica (2° rotation).

convenient to measure the u- and v-fields Moiré fringe patterns without moving the specimen.

(4) The AFM nano-Moiré pattern can be generated using atomic lattice and a 10 or 20 micron piezo-scanner. While AFM micro-Moiré patterns were formed using a 100 micron piezo-scanner and micro- and sub-micron spacing gratings.

In this study, with a mica sample, a 2° rotation a AFM nano-Moiré is generated by the interference of the atomic lattice of mica and AFM probe scan. This nano-Moiré pattern are shown in Fig. 10, which was recorded under the condition of scan line number $L = 79$ nm, and scan size $N = 128$.

(5) The AFM Moiré method has better resolution of observation than that of the electron beam Moiré method and the SEM scanning Moiré method, laser Moiré interferometer. A comparison among these methods is illustrated in Table 2. From Table 2, the applicable grating for AFM Moiré method strides across nanometer to micron spacing gratings. The experimental results from this study show that the AFM Moiré method has capability of measuring deformation in both nano- and micro-scale.

(6) The sign of the direct strain components ε_x, ε_y in Eqs. 9 and 10 can be judged using the rotating the reference grating method [9,10]. The sign of the partial derivative components $\partial u/\partial y$, $\partial v/\partial x$ in Eq. (11) can be easily determined according to the tangential angle of the Moiré fringe with respect to x-axis and the sign of the direct strain $\varepsilon_x, \varepsilon_y$ [9,10].

4. Conclusions

(1) The available results from this study verify the AFM Moiré method can be used in the deformation measurement in both micro- and nano-scale.

(2) In principle, the upper limit of utilized grating for this method can be atomic resolution, when a suitable piezo-scanner is utilized. From the results in this study, this method shows its capability of measuring the deformation in both nano- and micro-scales.

(3) The AFM Moiré method keeps the all the advantages of conventional Moiré method like full field, high sensitivity method for in-plane deformation measurement. The AFM scanning Moiré method has the extra advantages over conventional Moiré method on the aspect of high resolution for observation. Additionally, by mechanically translating the AFM stage, it is convenient to measure the deformation in different area. Besides, the measured area can be easily increased or decreased by changing the scan size (function of zoom-in or zoom-out). This is one special advantage of this method.

(4) The thermal deformation of the solders in a BGA electronic packages was measured. The shear strain components at the different solders in the packages were obtained. The result was compared with that from electron beam Moiré method. The comparison verifies that the results from two methods are consistent.

Table 2
A comparison among the different Moiré methods

Moiré method	Surface requirement	Applicable specimen grating (pitch)	Measurable size	Reference grating
AFM scanning Moiré	Conductive or non-conductive surface	From 0.1 nm to 2 μm	From 50 nm to 200 μm nano- to micro-scale	Continuously adjustable
Laser Moiré interferometry [1]	Reflective surface	With a $\lambda = 632.8$ nm He–Ne laser, from 0.32 to 1.67 μm	From 100 μm to few centimeter micro- to macro-scale	1200 lines/mm, 2400 lines/mm, 4800 lines/mm
Electron beam Moiré [3,4]	Conductive surface for non-conductive surface with accelerating voltage <1 kV	From 5 nm to 25 μm	From 50 μm to 5 mm micro- to macro-scale	Continuously adjustable
SEM scanning Moiré [2,5]	Conductive surface for non-conductive surface with accelerating voltage less than 1 kV	From 5 nm to 4 μm	From 50 μm to 5 mm micro- to macro-scale	Adjustable according to magnification and scan line number

(5) From the result, it illustrates the AFM Moiré method is effective tool in the failure analysis of electronic package, and will find more application in the design of electronic package. Additionally, this method can be extended to measure the deformation in the IC components, and will make more contribution to the reliability analysis of micro-electronic components.

References

[1] Post D, Han B, Ifju P. High sensitivity Moiré. New York: Springer-Verlag; 1994.
[2] Morimoto Y, Hayashi T. Deformation measurement during powder compaction by a scanning Moiré method. Exp Mech 1984;24(2):112–6.
[3] Read DT, Dally JW. Theory of electron beam Moiré. J Res Natl Inst Stan 1996;101(1):47–61.
[4] Xie H, Kishimoto S, Shinya N, Fulong D, Zou D, Liu S. Thermal deformation measurement of the solder joints in electronic package using electron Moiré method. Strain 1999;35(4):127–30.
[5] Xie H, Boay CG, Asundi A. Thermal deformation measurement of electronic package using advanced Moiré methods. In: The 3rd Electronics Packaging Technology Conference, 5–7 December, Singapore, IEEE Catalog No. 00EX456, 2000. p. 163–8.
[6] Xie H, Kishimoto S, Adundi A, Boay CG, Shinya N, Yu J, Ngoi BKA. In-plane deformation measurement using the atomic force microscope Moiré method. Nanotechnology 2000;11(1):24–9.
[7] Chen H, Liu D, Lee A. Moiré in atomic force microscope. Exptal Tech 2000;24(1):31–2.
[8] Lu YG, Zhong ZW, Yu J, Xie HM, Ngoi BKA, Chai GB, et al. Thermal deformation measurement of electronic packages using the atomic force microscope scanning Moiré technique. Rev Sci Instrum 2001;72(4):2180–5.
[9] Chiang F-P. Moiré methods of strain analysis. In: Doyle JF, Philips JW, editors. Manual on experimental stress analysis. 5th ed. Bethel, Connecticut: Society for Exp Mech; 1989.
[10] Durelli AJ, Parks VJ. Moiré analysis of strain. Englewood Cliffs, New Jersey: Prentice-Hall; 1970.
[11] Wiesendanger R. Scanning probe microscopy and spectroscopy: methods and applications. Cambridge: Cambridge University Press; 1994.